



# MICROSTRUCTURE OF HAZ METAL OF JOINTS OF HIGH-STRENGTH STRUCTURAL STEEL WELDOX 1300

V.A. KOSTIN, G.M. GRIGORENKO, T.G. SOLOMIJCHUK, V.V. ZHUKOV and T.A. ZUBER

E.O. Paton Electric Welding Institute, NASU

11 Bozhenko Str., 03680, Kiev, Ukraine. E-mail: office@paton.kiev.ua

Investigation of weldability of high-strength WELDOX 1300 steel with more than 1300 MPa yield limit is conducted under joint Ukrainian-Polish project, in order to assess the prospects for its application in crane construction in Ukraine. The objective of the work consisted in investigation of initial microstructure of WELDOX 1300 steel in as-delivered condition, influence of welding thermal cycle parameters on it, as well as plotting the thermokinetic diagram of austenite decomposition in this steel. This will allow optimization of arc welding modes to ensure high performance of the metal of weld and welded joint as a whole. The work was performed with application of procedures of light metallography, scanning microscopy, simulation of austenite transformation in Gleeble 3800 system, and computational methods of investigation. It was established that the microstructure of high-strength WELDOX 1300 steel in as-delivered condition consists of bainite-martensite mixture with a large number of finely-dispersed (50–100 nm) differently directed acicular precipitates of carbides of niobium NbC, titanium TiC, and iron Fe<sub>3</sub>C. A diagram of austenite transformation in this steel was plotted, and characteristic temperatures with new phase formation were determined. It is shown that preheating temperature should not be lower than 150 °C, in order to prevent cold cracking in welding WELDOX 1300 steel. Results of this work can be used in development of new welding technologies. 10 Ref., 4 Tables, 7 Figures.

**Keywords:** *new steels, carbonitride strengthening, welding thermal cycle, Gleeble 3800, microstructure, bainite, martensite, acicular ferrite*

One of the main problems of development of modern mechanical engineering is improvement of technico-economic indices of machines, mechanisms and engineering facilities based on lowering of their specific metal content, and improvement of operational reliability and fatigue life. When solving this problem, new superstrong steels (with more than 1000 MPa yield limit) with increased values of mechanical and toughness properties have an important role. The need for steels with such high values of strength is connected to a certain extent to the need for fabrication of metal structures of high-capacity cranes (250 t and higher).

Abroad the telescopic booms of truck cranes are usually made of STE 960 steel. In Ukraine the analogs of this steel are 12KhGH3MAFD and 15KhGN2MAFYuch steels. At present investigation of weldability of high-strength steel WELDOX 1300 with more than 1300 MPa yield limit was started under joint Ukrainian-Polish project in order to assess the prospects for its application in local crane construction.

As a rule, high-strength steels are used to manufacture booms and rotary platforms in crane structures. Individual parts of these structures

are connected to each other using arc welding processes. The thus formed welded joints should be characterized by equivalent strength and high impact toughness.

The weakest area in welded joints of high-strength steels is the HAZ, as the structure and properties of metal in it can undergo significant changes under the impact of the welding thermal cycle (WTC). This occurs both as a result of grain growth, and because of formation of quenching structures, lowering their brittle fracture resistance.

It is well-known that steel microstructure and the nature of its change in the metal of weld and HAZ essentially influence mechanical properties, ductility, toughness, and cold resistance of the welded joint as a whole. However, the data available in publications on the features of structural changes in WELDOX 1300 steel are scarce and unsystematic [1–3].

In this connection, the objective of this work consisted in investigation of initial microstructure of WELDOX 1300 steel in as-delivered condition, and influence of WTC parameters on it, as well as in plotting a thermokinetic diagram of austenite decomposition of this steel, that will allow establishing the optimum welding modes, providing high performance of the welded joint and studying the features of microstructure for-



**Table 1.** Composition of studied steel WELDOX 1300, wt.%

Object of study	C	Si	Mn	Cr	Ti	Ni	Mo	Nb	V	Cu	N	S	P
Steel WELDOX 1300 (UK_Special Data Sheet)	0.25	0.50	1.40	0.80	0.02	2	0.70	0.04	0.08	0.10	0.01	0.005	0.020
Steel WELDOX 1300	0.241	0.204	0.92	0.48	0.004	1.27	0.35	0.021	0.02	0.02	–	0.005	0.009

**Table 2.** Carbon equivalent values for WELDOX 1300 steel

Sheet thickness, mm	Certificate		Experiment	
	CEV, %	CET, %	CEV, %	CET, %
8	0.63	0.40	–	–
10	0.65	0.42	0.65	0.42

*Note.*  $CEV = C + Mn/6 + (Cr + Mo + V)/5 + (Ni + Cu)/15$ ;  $CET = C + (Mn + Mo)/10 + (Cr + Cu)/20 + Ni/40$ .

mation in the metal of weld and HAZ of this steel.

Composition of studied WELDOX 1300 steel in as-delivered condition and its comparison with those stated in the certificate (WELDOX\_1300\_UK\_Special Data Sheet: 2005-10-150) are given in Table 1.

High-strength steel WELDOX 1300 contains a large number of alloying elements, so that weldability is an urgent problem for it. Calculated and experimental values of carbon equivalent, depending on sheet thickness, are given in Table 2.

By the level of carbon equivalent this steel can be classified as steel with limited or poor weldability [4].

Mechanical properties of WELDOX 1300 steel stated in the certificate and determined experimentally, and weld metal properties are given in Table 3.

Investigations showed that the yield limit (about 1200 MPa) and ultimate strength (about 1600 MPa) of studied steel WELDOX 1300 are

approximately by 50–100 MPa lower than those stated in the certificate. As a result, characteristics of relative elongation (about 15 %) and reduction in area (61 %) increase 2 times at increase of impact toughness values.

Metallographic examination was performed using light microscope Neophot-32 at  $\times 500$  magnification and Auger-microprobe 9500F with high resolution field emission cathode in scanning electron microscope mode. Microstructure was revealed by etching in nital (4 % solution of nitric acid in alcohol). Vickers hardness measurement was conducted in the LECO hardness meter M-400 at 1 kg load. Calculation of structural components was performed by the field method to GOST 8233–56.

Initial microstructure of WELDOX 1300 steel is a bainite-martensite mixture (Figure 1, a), which consists approximately from 60–65 % of bainite and 35–40 % of martensite. Vickers hardness of base metal is equal to  $HV1-3780-3880$  MPa.

Microstructural features of WELDOX 1300 steel in as-delivered condition were studied using Auger-microprobe 9500F with high resolution field emission cathode. It was shown that initial structure of WELDOX 1300 steel consists of uniformly distributed grains of bainite and martensite (9–10 grain point; Figure 1, b) with a large quantity of finely-dispersed carbide precipitates. Bainite packets are located mainly along the grain boundary, whereas martensite ones are in the grain bulk, that is related to development of austenite decomposition kinetics from the

**Table 3.** Mechanical properties of WELDOX 1300 steel and weld metal

Object of study	$\sigma_{0.2}$ , MPa	$\sigma_t$ , MPa	$\delta_5$ , %	$\psi$ , %	KCV, J/cm <sup>2</sup> , at T, °C	
					–40	–60
WELDOX 1300 (UK_Special Data Sheet)	1300	1700	8	37.9	27	27
WELDOX 1300 (base metal)	1157	1605	16.0	61.2	33	–
	1205	1604	15.6	61.4		
	1253	1602	14.6	60.5		
WELDOX 1300 (weld metal)	818*	1047*	13.3*	43.7*	21**	–
	763*	1009*	10.0*	46.2*		
	801**	953**	3.7**	9.8**		

\*Testing was conducted on samples with preheating temperature of 150 and \*\*120 °C.

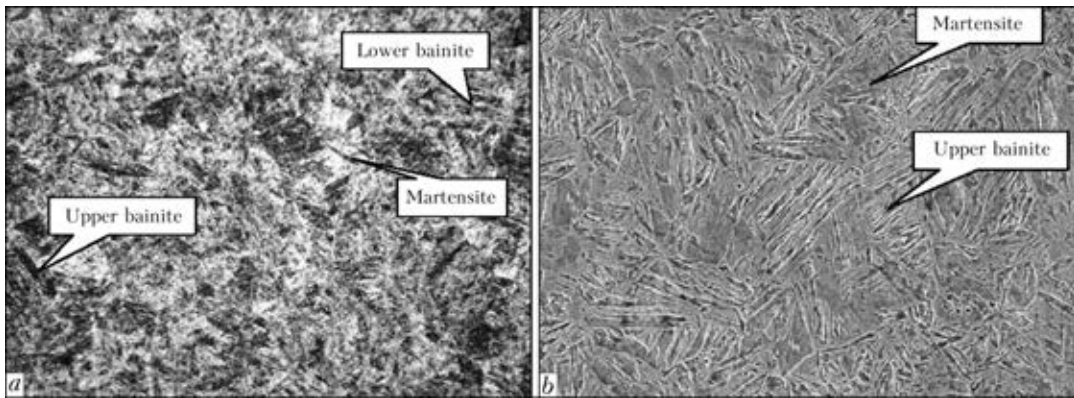


**Figure 1.** Microstructure of WELDOX 1300 steel in as-delivered condition: *a* – light microscopy ( $\times 500$ ); *b* – scanning microscopy ( $\times 2000$ )

boundaries towards the center of primary austenite grains.

Nature of carbide arrangement (Figure 2) in the bulk of bainite needles is indicative of the fact that lower bainite structure predominantly forms in these regions that is characterized by a favourable combination of strength and toughness properties. It is found that carbides have an acicular structure with needle dimensions of 50–100 nm. Proceeding from the data of X-ray structural analysis it was found that carbides of iron  $\text{Fe}_3\text{C}$  (in the amount of 0.52 %) and niobium  $\text{NbC}$  (0.04 %), and nitrides of aluminium  $\text{AlN}$  (0.01 %) and boron  $\text{BN}$  (0.01 %) form in the initial metal of WELDOX 1300 steel. Obtained data are in good agreement with those presented in [1]. Comparing the composition and nature of carbide precipitation in high-strength steels WELDOX 1300 and WELDOX 900, and using the method of electrolytical precipitation of carbides as a result of anode dissolution, the authors of the above work found that in WELDOX 900 steel strengthening is provided by nitrides of aluminium  $\text{AlN}$  and boron  $\text{BN}$ , whereas niobium carbides  $\text{Nb}_4\text{C}_{3.92}$  additionally form in WELDOX 1300 steel. Absence of iron carbides in the metal studied by the authors is, probably, related to dissolution of carbides of this type at anode dissolution.

To study the influence of WTC on HAZ metal structure, dilatometric investigations were performed and thermokinetic diagram of austenite transformation in WELDOX 1300 steel was plotted. Investigations were performed in Gleeble 3800 system, which allows simulation of thermodeformational cycle of welding on small diameter samples. For this purpose, samples of 6 mm diameter and 86 mm length were heated in a high-speed dilatometer up to 1350 °C at the rate of 150 °C/s, and then cooled in keeping with welding thermal cycles. During investigations the rate of metal cooling  $w_{6/5}$  was changed

from 1.3 up to 63 °C/s in the temperature range of 600–500 °C, that reproduces the main modes of arc welding of high-strength steels.

Processing of the results of dilatometric analysis and diagram plotting were performed by the generally accepted procedure. Quantitative analysis of the ratio of transformation products was conducted by dilatometric curves by the segment method [5].

In samples of WELDOX 1300 steel, in which structural transformations occur, the change of dimensions of dilatometric samples proceeds non-monotonically – metal expansion at the stage of its heating slows down (or is even replaced by compression), because of its contraction during  $\alpha \rightarrow \gamma$  transformation. At the cooling stage, contrarily, metal contraction is interrupted, because of its expansion in the temperature range of bainite-martensite transformations, which are completely over at temperatures below 150 °C and lead to development of high structural deformations.

Influence of cooling rate on austenite transformation temperature and HAZ metal microstructure is usually represented by thermokinetic diagram of austenite transformation. Proceeding from the results of dilatometric and metallographic analysis of simulator-samples, a ther-

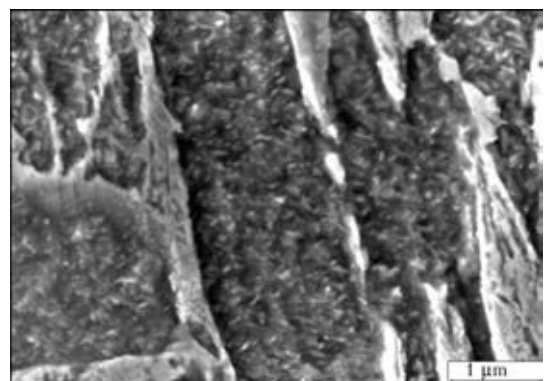


**Figure 2.** Microstructure of bainite grains

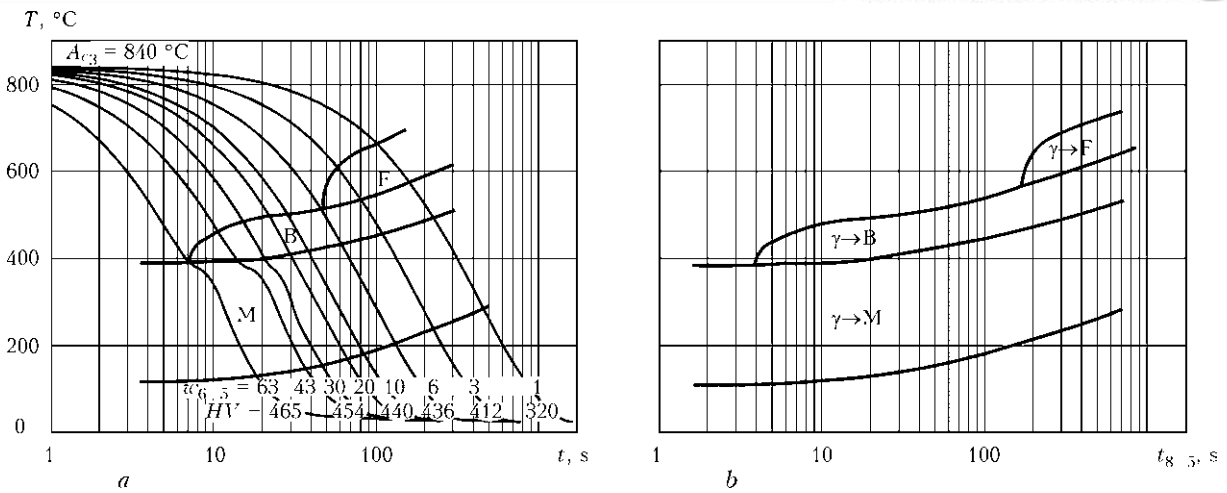


**Figure 3.** Thermokinetic diagrams of austenite decomposition for WELDOX 1300 steel: *a* – traditional; *b* – in temperature–cooling time  $t_{8/5}$  coordinates

mokinetic diagram of austenite transformation of WELDOX 1300 steel was plotted (Figure 3).

Austenite transformation in the studied range of cooling rates (from 1.3 up to 63 °C/s) occurs in the ferritic, bainitic and martensitic regions (Figure 3, *a*). At low cooling rates from 1.3 up to 6 °C/s, ferrite (F), bainite (B) and martensite (M) transformations will take place in HAZ metal of WELDOX 1300 steel. Solid solution alloying by molybdenum (0.8 %) and nickel (2 %) causes higher austenite stability, that results in the temperature of the start of ferrite transformation (at cooling rates of 3–5 °C/s) in this steel reaching extremely low values ( $F_s$  – of about 610–550 °C). With increase of cooling rate the quantity of ferrite gradually decreases and at 6 °C/s it disappears completely, and the structure consists of bainite and martensite.

Further increase of cooling rate up to 63 °C/s promotes intensive martensite transformation due to suppression of bainite transformation.

In the entire considered range of cooling rates ( $w_{6/5} = 1.3\text{--}63$  °C/s) temperature of the start  $M_s$  and end  $M_e$  of martensite transformation gradually decreases, with  $M_s$  temperature decreasing to a smaller degree (from 520 to 390 °C) than  $M_e$  temperature (from 290 to 110 °C) (Figure 3, *b*). Sample hardness rises from *HV* 320 up to *HV* 465.

At higher cooling rates ( $w_{6/5} > 63$  °C/s) a purely martensitic structure forms, and tempera-

ture of the start and end of structural transformations and hardness remain practically the same. With increase of the rate of cooling of WELDOX 1300 steel, the start and end of martensite transformations change in temperature range of 610–290 and 490–130 °C, respectively, and this leads to increase of martensite fraction in it from 35–40 up to 90–95 %. This steel is characterized by completion of the processes of austenite transformation – no residual austenite forms.

Increased content of alloying elements in WELDOX 1300 steel leads to a marked increase of  $M_s$  temperature of 520–390 °C (Figure 3, *b*). Comparison of calculated value ( $M_s = 480$  °C) of temperature of the start of martensite transformation with experimental data showed their quite good agreement in the region of low cooling rates:

$$M_s \text{ (}^\circ\text{C)} = 650 - 361C - 39Mn - 35V - 20Cr - 17Ni - 10Cu - 5Mo - 5W + 16Co + 30Al. \quad (1)$$

Thus, in order to obtain an equivalent joint of base and HAZ metal, it is necessary for cooling rate  $w_{6/5}$  to be higher than 6 °C/s. This cooling rate is in good agreement with the cooling rate recommended for welding high-strength steel with yield limit above 700 MPa, which, in the opinion of authors of [6], should be equal to  $10 \leq w_{6/5} \leq 20$  °C/s.

Having determined the optimal cooling rate of welded joint of WELDOX 1300 steel, appropriate process and modes of welding were se-

**Table 4.** Composition of weld metal of WELDOX 1300 steel and welding wire, wt.%\*

Object of study	C	Si	Mn	Cr	Ti	Ni	Mo	S	P
Flux-cored wire MEGAFIL-1100M	0.07	0.50	1.50	0.80	–	2.70	0.80	0.015	0.015
WELDOX 1300 weld	0.241	0.204	0.92	0.48	0.01	1.27	0.35	0.005	0.01

\*Nb, V ≈ 0.02 %, N = 0.06 %.

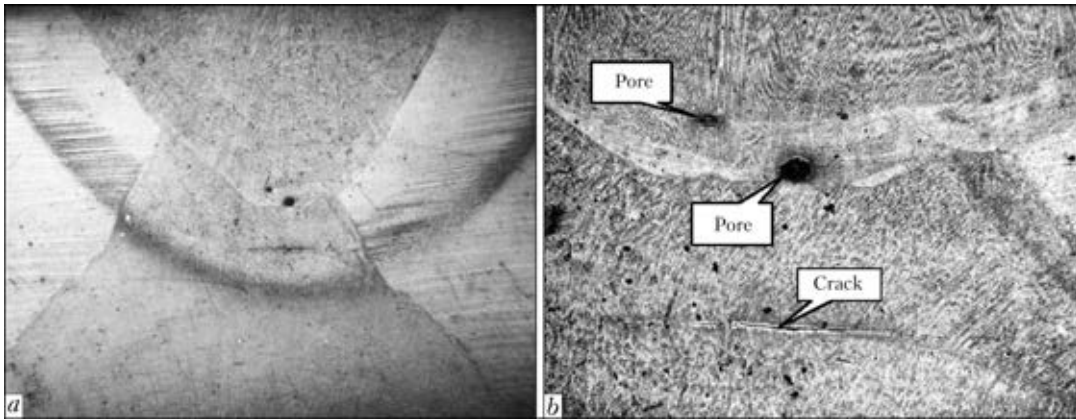


**Figure 4.** Macrostructure of weld on WELDOX 1300 steel: *a* – general view ( $\times 10$ ); *b* – cold cracks and pores in HAZ metal region ( $\times 50$ )

lected. Mechanized arc welding was conducted in argon with addition of  $\text{CO}_2$  gas (in the proportion of 82/18), respectively, with application of martensite type flux-cored wire MEGAFIL-1100R in the following mode:  $I_w = 250$  A,  $U_w = 30$  V,  $v_w = 14$  m/h.

Composition of weld metal and flux-cored welding wire is given in Table 4.

In order to avoid the possibility of cold cracking in welding WELDOX 1300 steel, preheating of plates to be welded was applied. Preheating temperature [7], which was calculated by equation (2), was equal to  $120$  °C:

$$T = 350\sqrt{[CE_{\text{tot}}] - 0.25}, \text{ } ^\circ\text{C}; \quad (2)$$

$$CE_c = \%C + \%Mn/6 + (\%Ni + \%Cu)/15 + (\%Cr + \%Mo + \%V)/5, \quad (3)$$

where  $CE_{\text{tot}}$  is the total carbon equivalent which is determined by expression  $CE_{\text{tot}} = CE_c + CE_s$ ;  $CE_c$  is the carbon equivalent dependent on metal composition, calculated by formula (2);  $CE_s$  is the carbon equivalent dependent on metal thickness, which is calculated by formula  $CE_s = 0.0058CE_c$  ( $\delta$  is the thickness of metal of welded part, mm).

Macrostructure of welded joint of WELDOX 1300 steel is given in Figure 4, *a*. Investigations showed that at preheating temperature of  $120$  °C individual microcracks of limited length (up to  $100$   $\mu\text{m}$ ) form in the zone of lower weld reheating (Figure 4, *b*). In our opinion, this circumstance accounts for lowering of weld metal ductility observed in joints of WELDOX 1300 steel in welding with preheating up to  $120$  °C. This leads to lower values of yield limit (801 MPa), strength (953 MPa) and ductility (3.7 and 9.8 % for relative elongation and reduction in area, respectively) of weld metal of steel WELDOX 1300 (see Table 3).

Increase of preheating temperature up to  $150$  °C leads to complete absence of cracks or

defects in the welded joint of WELDOX 1300 steel and to increase of yield limit (up to 1050 MPa) and ductility (13.3 and 43.7 % for relative elongation and reduction in area, respectively) of weld metal of WELDOX 1300 steel. Comparatively low values of mechanical properties of welds on WELDOX 1300 steel, compared to base metal properties, are related to absence of welding wires of sufficient strength in the world practical experience that would promote ensuring equivalent strength and cold resistance of welded joints of WELDOX 1300 steel.

Formation of cold cracks in the zone of crossing of two welds (Figure 4, *a*) is, apparently, related to the processes of carbide phase dissolution at reheating, at which the carbide forming elements (vanadium, molybdenum, niobium), but primarily carbon, go into the solid solution, causing considerable embrittlement of the matrix in this region. At cooling, increase of martensite lattice parameters leads to increase of local internal stresses, and their interaction with residual welding stresses leads to microcrack formation. This is indicated by the results of investigations, performed using computational methods by simulation of the processes of carbide phase dissolution in weld metal and HAZ during welding of WELDOX 1300 steel. This was performed using a computer program simulating phase transformations in metal systems at heating and cooling.

Calculation results on kinetics of the change of volume fraction and dimensions of carbide and nitride phases in the regions of HAZ metal of WELDOX 1300 steel, heated up to  $1400$  and  $1200$  °C with subsequent cooling at the rate of  $10$  °C/s, are shown in Figure 5.

Analysis of obtained results shows that depending on the applied WTC, processes of dissolution of carbide and nitride phases can proceed in characteristic regions of HAZ metal, strengthening WELDOX 1300 steel in as-delivered condition.

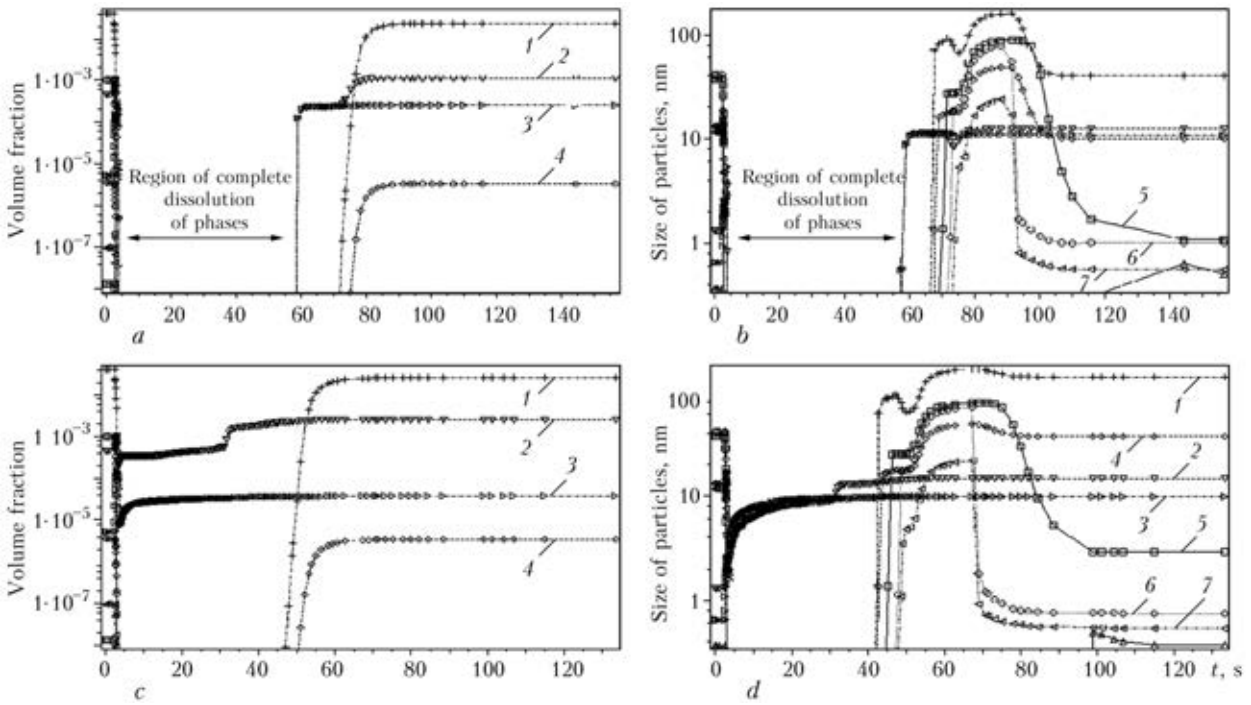


**Figure 5.** Design kinetics of variation in time of volume fraction (*a, c*) and dimensions (*b, d*) of carbide and nitride phases in HAZ regions of WELDOX 1300 steel heated up to 1400 (*a, b*) and 1200 (*c, d*) °C with subsequent cooling at  $w_{6/5} = 10$  °C/s: 1 – NbC; 2 – TiN; 3 – TiC; 4 – Fe<sub>3</sub>C; 5 – Me<sub>23</sub>C<sub>6</sub>; 6 – Me<sub>7</sub>C<sub>3</sub>; 7 – Me<sub>6</sub>C<sub>3</sub>

At maximum heating temperature of HAZ metal region (coarse-grained) complete dissolution of carbides of strengthening phases, namely TiC, NbC, Fe<sub>3</sub>C and nitride AlN can take place (Figure 5, *a, b*). In the fine-grained region, in which heating temperature does not exceed 1200 °C, nitrides and carbides of titanium TiC and TiN do not dissolve during the entire welding cycle (Figure 5, *c, d*).

It is well-known [8] that titanium nitrides TiN are almost insoluble in austenite. Computer simulation results obtained by us are in good agreement with the experimental results, given in [9], in which the temperatures of particle dissolution in austenite are 1350 (AlN), 1150 (NbC) and 1250 °C (TiC), respectively.

Investigation of microstructure of welded joint of WELDOX 1300 steel was conducted in

the central part of outer weld and its HAZ. Cast structure of the studied weld consists of columnar crystallites of different width. In the weld central part crystallite width changes from 20 up to 70 μm, and in the weld root the crystallites are much narrower: their width is equal to 10–15 μm.

Nature of Vickers hardness distribution across the section of welded joint of WELDOX 1300 steel is shown in Figure 6.

Upper weld microstructure (Figure 7, *a*) consists of dispersed interlaced ferrite needles or plates, oriented at angles of 60 and 90° relative to each other, with finely-dispersed carbide precipitates located along their boundaries. In its appearance such a structure is similar to acicular ferrite structure, forming in weld metal in welding of high-strength low-alloyed steels.

It is known that acicular ferrite forms as a result of transformation of inner regions of

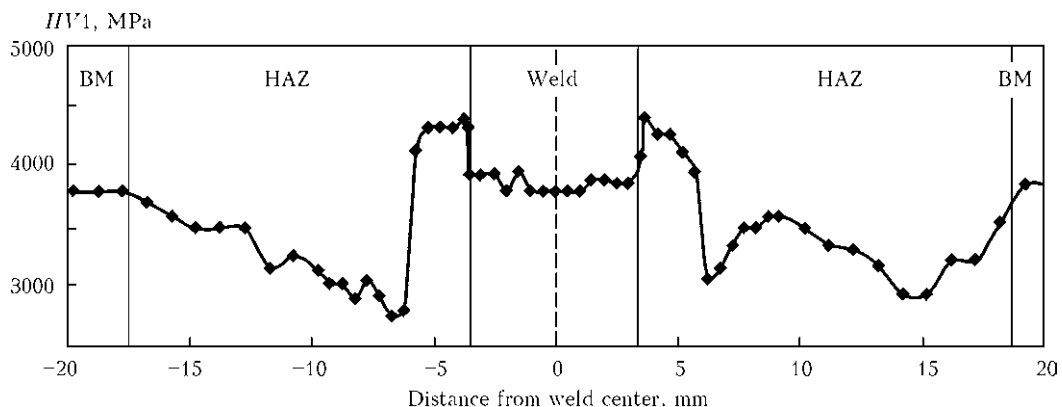


**Figure 6.** Hardness distribution across the section of the WELDOX 1300 steel welded joint

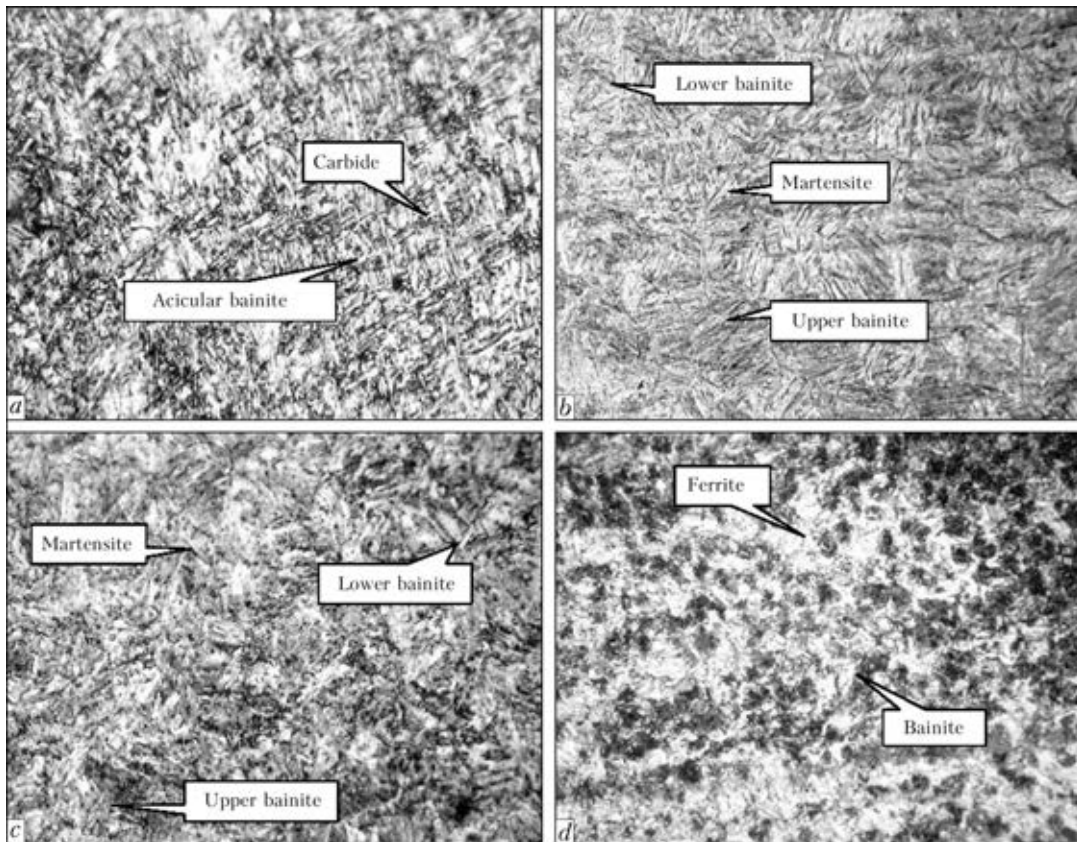


**Figure 7.** Microstructure ( $\times 1000$ ) of weld metal and HAZ of WELDOX 1300 steel made with application of MEGAFIL-110R wire: *a* – weld; *b* – coarse-grained region; *c* – fine-grained region; *d* – incomplete recrystallization region

austenite grains in the temperature range, which is only slightly higher than that of bainite transformation. Acicular ferrite is characterized by quite distinct features: these are fine elongated grains ( $1\text{--}3\ \mu\text{m}$ ) of a not quite regular shape with length to width ratios from 2:1 to 4:1. In upper weld microstructure the needles are much longer with 10:1 and greater ratio of length to width. In addition, Vickers hardness of such a structure is equal to  $HV1\text{--}3780\text{--}3950\ \text{MPa}$ , whereas hardness of «regular» acicular ferrite in the metal of welds of low-alloyed steels is equal to  $HV1\text{--}2400\text{--}2500\ \text{MPa}$ .

In this connection, the upper weld structure can be characterized as «acicular bainite», with needle arrangement in the form of «basket weave» characteristic of acicular ferrite [10].

Microstructure of coarse-grained region of HAZ metal (Figure 7, *b*) consists of structures of upper and lower bainite and martensite. In this region of welded joint hardness increase up to  $HV1\text{--}4320\text{--}4400\ \text{MPa}$  is observed. Fine-grained region also consists of bainite-martensite structure (Figure 7, *c*). Hardness of this region is somewhat lower than that of the coarse-grained region and is equal to  $HV1\text{--}3950\text{--}4130\ \text{MPa}$ . Hardness lowering in incomplete recrystallization region to  $HV1\text{--}2740\ \text{MPa}$  is related to the fact that a softer structural component, namely

ferrite, forms in the structure of this zone (Figure 7, *d*). Apparently, the rate of metal cooling in incomplete recrystallization region did not exceed  $6\ ^\circ\text{C}/\text{s}$  (see Figure 3, *a*), and this is exactly what led to formation of a large quantity (more than 50 %) of ferrite grains.

Lower hardness of welded joints of WELDOX 1300 steel made by flux-cored wire MEGAFIL-1100R in the atmosphere of shielding gases  $\text{Ar} + \text{CO}_2$  is due to the action of a number of factors, namely: formation of grains with ferrite structure of lower hardness ( $HV1\text{--}2740\text{--}3000\ \text{MPa}$ ) in incomplete recrystallization region; dissolution of dispersed phases ( $\text{Fe}_3\text{C}$ ,  $\text{NbC}$ ,  $\text{TiC}$ ), which levels the effect of carbide and carbonitride (dispersion) hardening; dissolution and transition of carbide-forming elements and carbon into the solid solution that increases the risk of cold cracking.

## Conclusions

1. Studying the microstructure of high-strength steel WELDOX 1300 in as-delivered condition showed that the initial steel microstructure consists of bainite-martensite mixture (about 60 % of bainite and 40 % of martensite). Bainite needles contain a large number of finely-dispersed ( $50\text{--}100\ \text{nm}$ ) differently oriented acicular pre-



cipitates of carbides of niobium NbC, titanium TiC and iron Fe<sub>3</sub>C (cementite).

2. A diagram of austenite transformation in new structural steel WELDOX 1300 was plotted, and it was found that at up to 6 °C/s cooling rates austenite transformation partially occurs in the diffusion region with formation of ferrite grains, whereas at increase of this cooling rate transformation runs in the region of intermediate and quenching structures.

3. Temperature of the start M<sub>s</sub> and end M<sub>e</sub> of austenite transformation gradually decreases, M<sub>s</sub> temperature decreasing to a smaller degree (from 520 to 390 °C) than M<sub>e</sub> temperature (from 290 to 110 °C). With increase of cooling rate of WELDOX 1300 steel, the start and end of bainite-martensite transformations changes in the temperature range of 610–290 and 490–130 °C, respectively, and leads to increase of martensite fraction in it from 35–40 up to 90–95 %, respectively.

4. It is found that the cause for low mechanical properties of welded joints of WELDOX 1300 steel is associated with formation of cold cracks in the region of reheating of the lower weld as a result of dissolution of carbide and nitride phases (Fe<sub>3</sub>C, TiN, TiC). Preheating temperature of 120 °C is insufficient to prevent cold cracking. At preheating temperature of 150 °C no mi-

crocracks or defects form in the weld metal of WELDOX 1300 steel.

1. Ozgovicz, W., Kurc, A., Nawrat, G. (2008) Identification of precipitations in anodically dissolved high-strength microalloyed Weldox steels. *Archives of Materials Sci. and Eng.*, **31**, 95–100.
2. Welding Hardox and Weldox. <http://www.ssab.com>
3. Ozgovicz, W., Kalinowska-Ozgowicz, E. (2008) *Investigations on the impact strength of constructional high-strength Weldox steel at lowered temperature*. Vol. 32, 89–94.
4. (1974) *Reference book of welder*. Ed. by V.V. Stepanov. Moscow: Mashinostroenie.
5. Steven, W., Mayer, G. (1953) Continuous-cooling transformation diagrams of steels. Pt 1. *J. Iron and Steel Inst.*, **174**, 33–45.
6. Zhdanov, S.L., Mikhoduj, L.I., Strizhak, P.A. et al. (1994) Structural transformations in welding of 17Kh2M steel and properties of welded joints. *Avtomatich. Svarka*, **9/10**, 10–13.
7. Seferian, D. (1963) *Welding metallurgy*. Moscow: Metallurgizdat.
8. Gorbachev, I.I., Popov, V.V. (2009) Analysis of solubility of carbides, nitrides and carbonitrides in steels by computer-assisted methods of thermodynamics. Pt 3: Solubility of carbides, nitrides and carbonitrides in Fe-Ti-C, Fe-Ti-N and Fe-Ti-C-N systems. *Fizika Metallov i Metallovedenie*, **108(5)**, 513–524.
9. Hrivnak, I. (1969) The study of the system Fe-V-C-N with a view to the precipitation hardening process. *Czech. J. Physics*, **19**, 287.
10. Grabin, V.F., Denisenko, A.V. (1978) *Metals science of low- and medium-alloy steels*. Kiev: Naukova Dumka.

Received 25.12.2012

## NEWS

### *Testing of Compensation Devices in Systems of Transportation of Heat Carriers*

At the E.O. Paton Electric Welding Institute the equipment has been designed and procedure has been developed for testing the telescopic compensators of heat systems, allowing evaluation of efficiency and serviceability of accepted design solutions; evaluating their service life under the conditions of loadings, simulating the complex of loads exceeding the planned term of service of products. Simultaneously, the testing of two compensators are carried out, which were assembled and mounted on the stand so that one of them was fixed in a stretched state, and another one – in a compressed state. Owing to this scheme the volume of internal cavity of the compensator remains unchanged in testing during the process of movement of branch pipe relative to a casing. Stand is equipped by a hydraulic system for

creation of excessive pressure of a required value inside the compensators, water heat source, and also a power system, providing a reciprocal movement of a mobile part of compensators at a preset speed, here the cyclic movement of a pipeline area is simulated. Compensators can be tested of different designs of diameter 200–800 mm at the following parameters: amplitude of movement is up to 250 mm; speed of movement is 0.5–6.0 cm/min; pressure of operating medium – preset; temperature of operating medium – up to 170 °C.

Using these tests, the optimizing of design of compensating devices and their welded elements, as well as evaluation and checking of their serviceability are made.